World Academy of Science, Engineering and Technology
International Journal of Mechanical and Mechatronics Engineering
Vol:9, No:10, 2015

Effect of Robot Configuration Parameters, Masses and Friction on Painlevé Paradox for a Sliding Two-Link (P-R) Robot

Hassan M. Alkomy, Hesham A. Elkaranshawy, Ahmed S. Ashour, Khaled T. Mohamed

Abstract**—**For a rigid body sliding on a rough surface, a range of uncertainty or non-uniqueness of solution could be found, which is termed: Painlevé paradox. Painlevé paradox is the reason of a wide range of bouncing motion, observed during sliding of robotic manipulators on rough surfaces. In this research work, the existence of the paradox zone during the sliding motion of a two-link (P-R) robotic manipulator with a unilateral constraint is investigated. Parametric study is performed to investigate the effect of friction, link-length ratio, total height and link-mass ratio on the paradox zone.

Keywords**—**Dynamical system, friction, multibody system, Painlevé paradox, robotic systems, sliding robots, unilateral constraint.

I. Introduction

DURING sliding of a rigid body on a rough surface, many unexpected behaviors could occur. A famous simple example is the periodic detachment of a piece of a chalk when it is pushed over a blackboard [1]. Such phenomenon can be generalized to any rigid body or multibody system performing sliding on a rough surface with a unilateral constraint and the mass center trails the contact point as a pushing motion. This configuration could result in a range of uncertainty or non-uniqueness of the solution of the equations of motion. Painlevé was the first who noticed this phenomenon and studied it [2], so it was named as Painlevé paradox [3]-[5]. He performed his studies on a planar rod slides on a rough surface. This model became the typical Painlevé model. The paradox in the typical Painlevé model may appear at a quite large value of the coefficient of friction, typically more than 4/3 [6] which are, mostly, not found in practical applications. In the same time, the bouncing motion is one of the most important problems affecting multibody systems like robots, because it represents an obscure during their desired motion trajectories. What deteriorates the situation is the fact that the Painlevé paradox may appear for multibody systems at much smaller values of the coefficient of friction depending on the system configuration [4], [6]-[8]. Hence, the Painlevé phenomenon becomes very important in practical applications. Several problems can be named such as self-locking and bouncing motion related to the Painlevé paradox phenomenon [4]-[6], [9]-[11]. Reference [6] studied deeply the typical Painlevé model and focused on the inconsistencies and the indeterminacies regions. He defined the motion modes and studied the transition from one mode to another one. Researchers in [4] and [11] made an experimental study on a two link robotic system with revolute joints in contact with a rough moving belt (to simulate the sliding motion) and they proved that the Painlevé paradox is a main reason for the undesired bouncing motion. They used the concept of tangential impact to solve the paradox analytically. Numerical simulation was carried out and numerical results showed good agreement with the experimental ones. A parametric study was performed [12] on a two link robot with revolute joints to study the effect of its configuration parameters on Painlevé phenomenon. The same authors in a following paper [13] suggested a method to escape Painlevé paradox by controlling the distance between the base of the robot and the ground. Reference [14] used the redundancy as a way to escape the paradox zone. He used a three-link redundant planar sliding robot with three actuated revolute joints to control the paradox and to escape its zone during motion. It can be noticed that these previous studies have considered either a single rod, as the typical Painlevé problem, or a two-link robot with revolute joints. Though in [14] a redundant robotic system with three links has been considered, however, all joints were revolute joints.

In this work, a two-link robot with one prismatic joint and one revolute joint, or simply (P-R) robot is considered and analyzed. A derivation of the dynamical model of a general multibody robotic system with a unilateral constraint is introduced. Next, the condition for the Painlevé paradox, in the form of a paradox index, is determined and analyzed and different states of solution are illustrated. The case study of the two-link robotic system with one prismatic joint is investigated. Numerical and parametric studies, on the chosen model, are presented. The effect of link parameters (length ratio, mass ratio and total height), and friction on the dynamical behavior of the system are demonstrated. The results are represented graphically and discussed in detail.

II. Dynamic System Modeling

For a planar robotic system in vertical plane, the end effector (contact point) is sliding on a rough horizontal surface. The coordinate components of the contact point *(x, y),* with respect to the inertial Cartesian coordinate frame $O_{x,y}$, can

H. M. Alkomy, H. A. Elkaranshawy, A. S. Ashour and K. T. Mohamed are with the Faculty of Engineering in Alexandria University, Alexandria, Egypt (e-mail: eng.alkomy@gmail.com, hesham_elka@hotmail.com, a.ashou77@gmail.com, ktawfik64@yahoo.com).

be expressed in terms of the generalized coordinates $\boldsymbol{q}(q_1,q_2,\ldots, q_n)$ as

$$x = x(\boldsymbol{q}) \tag{1}$$

$$y = y(\boldsymbol{q}) \tag{2}$$

In this case, the dynamical system can be obtained using Euler–Lagrange Equations, which produce the second order nonhomogeneous differential equation [12]:

$$\boldsymbol{\Phi}(\boldsymbol{q})\,\ddot{\boldsymbol{q}} + \boldsymbol{u}(\boldsymbol{q},\dot{\boldsymbol{q}}) = \boldsymbol{w} + \boldsymbol{f} \tag{3}$$

where, $\boldsymbol{q}$: Vector of generalized joint coordinates, $\boldsymbol{\Phi}(\boldsymbol{q})$: Inertia matrix, $\boldsymbol{u}(\boldsymbol{q},\dot{\boldsymbol{q}})$: Vector of Coriolis and centripetal forces, $\boldsymbol{w}$: Generalized active forces, $\boldsymbol{f}$: Generalized contact forces expressed with respect to joint coordinates. $\boldsymbol{f}$ can be written in terms of contact forces at the contact point as:

$$\boldsymbol{f} = \boldsymbol{J}^T \begin{bmatrix} F_n \\ F_t \end{bmatrix} \tag{4}$$

where, F_n is the normal component of the contact force, F_t is the tangential component of the contact force, $\boldsymbol{J}$ is the robot Jacobian, In sliding motion F_t can be written in terms of F_n as:

$$F_t = -\mu\sigma F_n \tag{5}$$

where, σ is sliding direction indicator which is given by:

$$\sigma = \frac{\dot{x}}{|\dot{x}|} \tag{6}$$

where, $\dot{x}$ is tangential (sliding) component of the velocity of the contact point. The Jacobian can be defined from:

$$\boldsymbol{v_c} = \boldsymbol{J}\dot{\boldsymbol{q}} \tag{7}$$

where, $\boldsymbol{v_c}$ is the velocity of the contact point, and

$$\boldsymbol{J} = \begin{bmatrix} \boldsymbol{\alpha}^T \\ \boldsymbol{\beta}^T \end{bmatrix} \tag{8}$$

Finally, the equation of motion can be written as:

$$\ddot{\boldsymbol{q}} = \boldsymbol{\Phi}^{-1}(\boldsymbol{w} - \boldsymbol{u}) + \boldsymbol{\Phi}^{-1}\boldsymbol{f} \tag{9}$$

III. Painlevé Paradox Modeling

Using (7) and (8), the velocity of the contact point can be expressed as:

$$\boldsymbol{v_c} = \begin{bmatrix} \dot{y} \\ \dot{x} \end{bmatrix} = \begin{bmatrix} \boldsymbol{\alpha}^T \\ \boldsymbol{\beta}^T \end{bmatrix} \dot{\boldsymbol{q}} \tag{10}$$

where, $\dot{y}$ is the normal component of the velocity of the contact point, it follows that:

$$\dot{y} = \boldsymbol{\alpha}^T\dot{\boldsymbol{q}} \tag{11}$$

Differentiating (11) and substitution (9) in the obtained equation leads to:

$$\ddot{y} = \left[\dot{\boldsymbol{\alpha}}^T\dot{\boldsymbol{q}} + \boldsymbol{\alpha}^T\boldsymbol{\Phi}^{-1}[\boldsymbol{w} - \boldsymbol{u}]\right] + [\boldsymbol{\alpha}^T\boldsymbol{\Phi}^{-1}[\boldsymbol{\alpha} - \mu\sigma\boldsymbol{\beta}]F_n] \tag{12}$$

or

$$\ddot{y} = -A + BF_n \tag{13}$$

where

$$A = -\dot{\boldsymbol{\alpha}}^T\dot{\boldsymbol{q}} - \boldsymbol{\alpha}^T\boldsymbol{\Phi}^{-1}[\boldsymbol{w} - \boldsymbol{u}] \tag{14}$$

$$B = \boldsymbol{\alpha}^T\boldsymbol{\Phi}^{-1}[\boldsymbol{\alpha} - \mu\sigma\boldsymbol{\beta}] \tag{15}$$

where B is called the paradox index.

Physically, there are two possibilities for motion: either regular sliding ($\ddot{y} = 0 \;,\; F_n > 0$) or flying ($\ddot{y} > 0 \;,\; F_n = 0$). This physical condition can be expressed mathematically using the following complementary condition:

$$\ddot{y} \geq 0 \quad , \quad F_n \geq 0 \quad and \quad \ddot{y}.F_n = 0 \tag{16}$$

Mathematically, depending upon the signs of A and B, four possibilities of solution can be obtained from (13) as:

a. The first possibility of solution occurs when A is positive and B is positive, which leads to:

$$\ddot{y} = 0 \;\;,\; F_n = \frac{A}{B} > 0 \tag{17}$$

This possibility of solution represents the regular sliding of the end effector and it is the first accepted possibility of solution.

b. The second possibility of solution occurs when A is negative and B is positive, which leads the solution to be as:

$$\ddot{y} = -A > 0 \;\;,\; F_n = 0 \tag{18}$$

This possibility of solution represents the case of flying (end effector leaves the surface) and it is the second accepted possibility of solution.

c. The third possibility of solution is when A is negative and B is negative which leads the solution to be as:

$$F_n = \frac{A}{B} > 0 \;\;, \qquad \ddot{y} = 0 \;\; and \;\; F_n = 0 \;\;, \qquad \ddot{y} = -A > 0 \tag{19}$$

In this case, the two accepted possibilities of solution (regular sliding and flying) are possible at the same time which is called indeterminacy or non-uniqueness. This possibility is rejected according to the mentioned physical condition and it is the first rejected possibility of solution.

d. The fourth possibility of solution happens when A is positive and B is negative. In this case, if $\ddot{y} = 0\; then\; F_n = \frac{A}{B} < 0$ is a mathematical solution which means that the normal reaction is directed towards the rough surface which is rejected. If $F_n = 0\; then\; \ddot{y} = -A < 0$ is another mathematical solution which means that the normal

component of acceleration is directed towards the rough surface which is rejected also. This case has no accepted solution which can be called inconsistency and this will be the second rejected possibility of solution.

It is clear that, the two accepted possibilities of solution can be found only when $B>0$. In cases of $B<0$ the two rejected possibilities of solution will be found. The type of the two rejected possibilities of solution is dependent, also, on the sign of the term A. When A is negative, the non-uniqueness will be found, however, when A is positive the inconsistency will be found.

Table I shows these cases according to the term A and term B signs. Hence, if B is positive a unique solution can be specified and contrarily, if B is negative, a range of inconsistency or non-uniqueness of solution can be occurred according to the sign of A. This phenomenon is called Painlevé paradox and we can define B as the paradox index. It is worth to notice from B-relation in (15) that B does not depend on the applied loads or motion velocities. It depends, only, upon the system configuration (orientation), mass properties (length, mass, specific mass), sliding direction, and coefficient of friction. Hence, for any specific coefficient of friction, a paradoxical configuration can be specified vice versa.

TABLE I
STATES OF SOLUTION

	A	B	Solution	State of solution
1	+	+	$F_n = \frac{A}{B} > 0$, $\ddot{y} = 0$	Sliding
2	-	+	$F_n = 0$, $\ddot{y} = -A > 0$	Flying
3	+	-	Φ	Inconsistency (no solution)
4	-	-	$F_n = \frac{A}{B} > 0$, $\ddot{y} = 0$ and $F_n = 0$, $\ddot{y} = -A > 0$.	Indeterminacy (non-uniqueness)

IV. CASE STUDY

Fig. 1 shows a two-link planar robotic system (two degrees of freedom) in the vertical plane, whose end effector C is sliding on a rough horizontal surface with coefficient of friction μ, and the first link can move vertically through the prismatic joint O. Assuming that l_1, l_2 are the lengths of the first and second links and m_1, m_2 are their respective masses. The vertical distance between the surface and the fixed prismatic joint is H. The motion parameters are the linear displacement d and the angular displacement θ which are chosen as the generalized coordinate $\boldsymbol{q}$. The applied force F acts at the prismatic joint (O) and τ is the applied torque at the revolute joint.

The kinetic energy of the robotic system is:

$$T = \frac{1}{2}m_1\dot{d}^2 + \frac{1}{8}m_2 l_2^2\dot{\theta}^2 + \frac{1}{2}m_2\dot{d}^2 - \frac{1}{2}m_2 l_2 \sin\theta\dot{\theta}\dot{d} + \frac{1}{2}I_{G2}\dot{\theta}^2 \qquad (20)$$

The potential energy of the robotic system is:

$$V = -Fd + m_1 g\left(\frac{l_1}{2} - d\right) + \tau\left(\frac{\pi}{2} - \theta\right) - m_2 g\left(d + \frac{l_2}{2}cos\,\theta\right) \qquad (21)$$

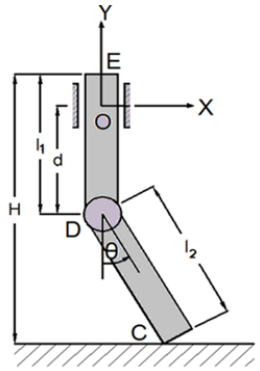

Fig. 1 Two-link (P-R) planar robotic manipulator

Consequently, using the model presented in Section II, the matrices and vectors in (9) are obtained as follows:

$$\boldsymbol{\Phi} = \begin{bmatrix} (m_1 + m_2) & -\frac{1}{2}m_2 l_2 sin\theta \\ -\frac{1}{2}m_2 l_2 sin\theta & \left(\frac{1}{4}m_2 l_2^2 + I_{G2}\right) \end{bmatrix} \qquad (22)$$

$$\boldsymbol{u} = \begin{bmatrix} -\frac{1}{2}m_2 l_2 \cos\theta\dot{\theta}^2 \\ -m_2 l_2 \cos\theta\dot{\theta}\dot{d} \end{bmatrix} \qquad (23)$$

$$\boldsymbol{w} = \begin{bmatrix} (m_1 + m_2)g + F \\ -\frac{1}{2}m_2 l_2 g sin\theta + \tau \end{bmatrix} \qquad (24)$$

$$\boldsymbol{f} = [\boldsymbol{\alpha} - \mu\sigma\boldsymbol{\beta}]F_n \qquad (25)$$

$$\boldsymbol{\alpha} = \begin{bmatrix} \alpha_1 \\ \alpha_2 \end{bmatrix} = \begin{bmatrix} -1 \\ l_2 sin\theta \end{bmatrix} \qquad (26)$$

$$\boldsymbol{\beta} = \begin{bmatrix} \beta_1 \\ \beta_2 \end{bmatrix} = \begin{bmatrix} 0 \\ l_2 cos\theta \end{bmatrix} \qquad (27)$$

Substituting (22), (26), (27) in (15), B can be written as:

$$B = \frac{6sin^2\theta - 4 + 6sin\theta(sin\theta - \mu\sigma cos\theta)}{3m_2 sin^2\theta - 4m_2 - 4m_1} + \frac{12sin\theta(sin\theta - \mu\sigma cos\theta)}{m_2(3m_2 sin^2\theta - 4m_2 - 4m_1)} \qquad (28)$$

Due to the unilateral constraint, the following relation is applicable:

$$H = d + l_2 \cos\theta \qquad (29)$$

where,

$$0 < H < (l_1 + l_2)$$

Substituting (29) in (28), another relation for B can be obtained as:

$$B = \frac{4l_2^2 - 12l_2^2\sqrt{1-\frac{(H-d)^2}{l_2^2}}\sqrt{\frac{-H^2+2Hd-d^2+l_2^2}{l_2^2}}}{3m_2H^2 - 6Hm_2d + 3m_2d^2 + 4m_1l_2^2 + m_2l_2^2} + \frac{6\mu\sigma l_2(H-d)\sqrt{\frac{-H^2+2Hd-d^2+l_2^2}{l_2^2}}}{3m_2H^2 - 6Hm_2d + 3m_2d^2 + 4m_1l_2^2 + m_2l_2^2} + \frac{(l_2\sqrt{1-\frac{(H-d)^2}{l_2^2}} - \mu\sigma(H-d))(12l_2(m_1+m_2)\sqrt{1-\frac{(H-d)^2}{l_2^2}})}{m_2(3m_2H^2 - 6Hm_2d + 3m_2d^2 + 4m_1l_2^2 + m_2l_2^2)} \quad (30)$$

Putting $B = 0$ in (28) leads to $B(\theta_1) = B(\theta_2) = 0$ which determine the paradox zone boundaries. $\forall\theta \in (\theta_1, \theta_2)$ leads to $B(\theta) < 0$ which means that the motion is in the Painlevé paradox zone. If θ_f is defined as the maximum possible value for θ to keep the touching between the robot end and the rough surface, then $\forall\, \theta \in [0, \theta 1) \cup (\theta 2\,, \theta \mathrm{f}]$ leads to $B(\theta) > 0$ and the motion is out from the Painlevé paradox zone, i.e. the solution is consistent and determined and the regular equations of motion (9) can be applied. It has to be noticed that Painlevé paradox occurs only when the center of mass trails the contact point [1], so in this research the motion of the robot was studied during one quadrant of its trajectory. In this quadrant σ =1 and the center of mass trails the contact point, so, d is downwards and θ is counter-clockwise as shown in Fig. 1.

V. Simulation and Parametric Study

To investigate the effect of link-length ratio, link-mass ratio, total height ratio and friction on the dynamical behavior of the system, a numerical analysis was conducted. The values of constants in all cases were: m_1 = 0.12 kg and l_1 = 0.21m. In Figs. 2-8, each curve represents the motion of the robot starting from $\theta = 0$ (or the corresponding value of d calculated from (29)) and ending at θ_f (or the corresponding value of d). The starting and ending positions of the paradox range, θ_1 and θ_2 (or d_1 and d_2), are specified by the intersection of each curve with the horizontal straight line B = 0.

A. The Effect of Link-Length Ratio (γ)

Let $m_1 = m_2$ = 0.12 kg, H = 0.3775 m, μ = 1 and the of link-length ratio $0.9 \le \gamma \le 1.7$, where $\gamma = l_2 / l_1$. The relation between θ and B is shown in Fig. 2. In this case, almost θ_1 = 17° and θ_2 = 39°. According to (28) the effect of γ on B cannot be seen in this figure since this effect is inherited in θ itself. One should consult (29) and subsequently (30) to grip the relation between γ and B. Consequently in Fig. 3, which shows the relation between d and B for a range of link-length ratios γ, it can be noticed that increasing the link-length ratio results in increasing the paradox region in terms of d and entering the paradox region at lower values of d.

B. The Effect of Link-Mass Ratio (δ)

Let $l_2 = l_1$ = 0.21, H = 0.3775 m, μ = 1, and the link-mass ratio $0.5 \le \delta \le 1.8$, where, $\delta = \frac{m2}{m1}$. Fig. 4 shows the variation of B with respect to θ at different link-mass ratios. It is clear that increasing the link-mass ratio δ decreases the paradox zone range and delays its occurrence. For higher δ, the robot can escape the paradox zone totally. A similar phenomenon can be seen in Fig. 5, which represents the variation of B with respect to d at different link-mass ratios. The two figures illustrate that there is a specific value δ^* (depends upon the configuration parameters of the robotic system) for $\delta > \delta^*$ the paradox zone will totally disappear.

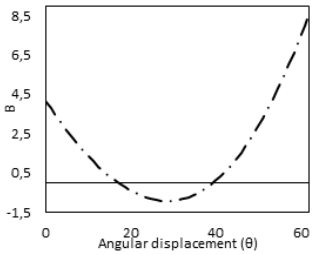

Fig. 2 Angular displacement (θ) vs. B for a range of $\gamma = l_2 / l_1$ ($m_1 = m_2 = 0.12$kg, $\mu = 1$)

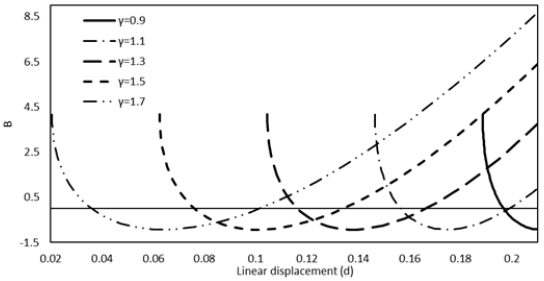

Fig. 3 Linear displacement (d) vs. B for a range of $\gamma = l_2 / l_1$ ($m_1 = m_2 = 0.12$kg, $H = 0.3775$, $\mu = 1$)

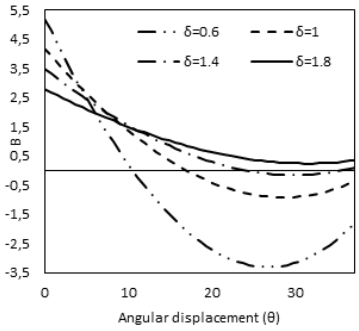

Fig. 4 Angular displacement (θ) vs. B for a range of $\delta = m_2 / m_1$ ($\mu = 1$)

C. The Effect of Total Height (H/l)

Assume that $l_2 = l_1 = l$ = 0.21, $m_1 = m_2$ =0.12 kg, μ = 1 and the total height $1.05 \le H/l \le 1.85$. According to (28) the relation between θ and B for the specified range of the total height is shown in Fig. 2 also. One should refer to (29), (30) to grasp the relation between H/l and B as can be seen in Fig. 6. For illustration, when H/l = 1.05 the robot enters the paradox region at d = 0.02 m, but when H/l = 1.25 the robot enters the region at d = 0.06 m, however for these two values of H/l the robot remains in the paradox region for approximately Δd = 0.04 m. Therefore, the arrival of the robot to the paradox zone varies according to the value of H/l but the range of the paradox zone in terms of d is unchanging.

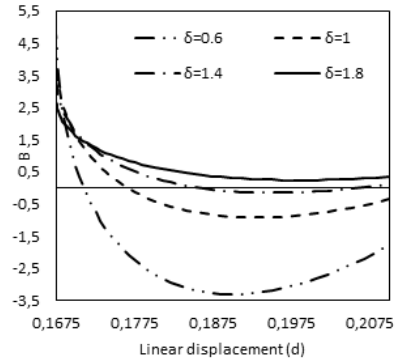

Fig. 5 Linear displacement (*d*) vs. B for a range of $\delta = m_2/m_1$ ($l_1 = l_2 = 0.21m$, $H = 0.3775$, $\mu = 1$)

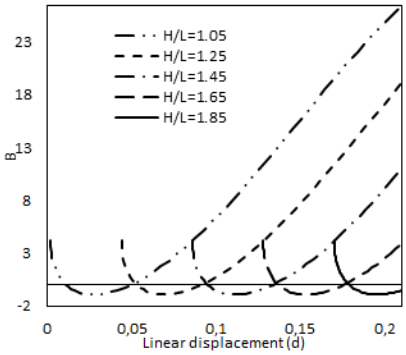

Fig. 6 Linear displacement (*d*) vs. B for a range of *H/l* ($m_1 = m_2 = 0.12kg$, $l_1 = l_2 = 0.21m$, $\mu = 1$)

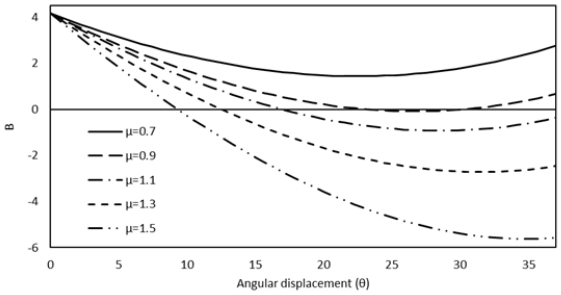

Fig. 7 Angular displacement (θ) vs. B for a range of μ ($m1 = m2 = 0.12\ kg$)

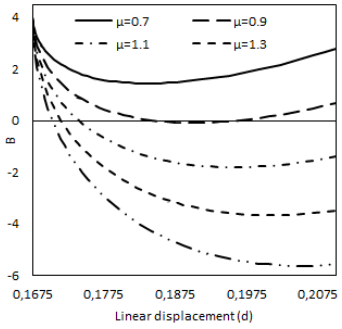

Fig. 8 Linear displacement (*d*) vs. B for a range of μ ($m1 = m2 = 0.12kg$, $l1 = l2 = 0.21m$, $H = 0.3775m$)

D. The Effect of Coefficient of Friction (μ)

Let $l_2 = l_1 = 0.21$, $m_1 = m_2 = 0.12$ kg, $H = 0.3775$ and the range for the coefficient of friction $0.7 \leq \mu \leq 1.5$. The coefficient of friction μ deeply affects the paradox region and the behavior of the robotic system. Higher μ leads to larger paradox zone, also, the robot enters the paradox zone at lower values for both θ and d, as shown in Figs. 7 and 8. The figures show that there is a critical value μ^*, which depends on the robot's mass and dimension parameters, if $\mu < \mu^*$ there will be no paradox zone. For the considered robot μ^* is slightly less than 0.9 which also represents the minimum value required for the coefficient of friction for the occurrence of Painlevé paradox. The paradox in the typical Painlevé model may appear at a quite larger value of the coefficient of friction, typically more than 4/3. From the practical point of view, the occurrence of Painlevé phenomenon becomes quite conceivable in practical robotic systems.

VI. Conclusion

In this research work, a dynamical model of a planar robotic system has been introduced. The equations of motion, of a two-link (P-R) robot, have been obtained using Euler-Lagrange method and the condition leading to Painlevé paradox, in the form of a paradox index, has been determined. Numerical parametric studies were conducted to investigate the effect of link-length ratio, link-mass ratio, total height and friction on the dynamical behavior of the system. The size of the paradox zone expands and it occurs at lower value for the linear motion displacement with the increase of the link-length ratio. Oppositely, the size of the paradox zone decreases and it occurs at higher value for motion parameters with increasing link-mass ratio. Increasing the total height does not affect the size of the paradox zone though the robot enters the zone at higher value for the linear motion displacement. The size of the paradox zone expands and it occurs at lower value for the motion parameters with the increase of the coefficient of friction. Generally, critical values to escape the paradox zone can be specified to link-mass ratio and friction coefficient. This research work illustrates that for this robotic system the Painlevé paradox could occur at practical values of the coefficient of friction. Through a parametric study, we indicate how to control the size of the paradox zone and even how to escape it.

References

[1] Benjamin Hall and Champneys, Alan (2009), "Why does Chalk Squeak?", Master thesis, University of Bristol.
[2] Painlevé, P. (1895), "Sur le Lois du Frottement de Glissement", Comptes Rendus Academie Science Paris, Vol. 121, 112-115.
[3] An, L. (1990), "The Painleve Paradox and the Law of Motion of Mechanical Systems with Coulomb Friction", PMM U. S. S. R., Vol. 54, (4), 430-438.
[4] Liu, C., Zhao, Z. and Chen, C. (2007), "The Bouncing Motion Appearing in the Robotic System with Unilateral Constraint", Nonlinear Dyn., Vol. 49, 217-232.
[5] Nordmarka, A., Dankowiczb, H. and Champneys, A. (2009), "Discontinuity Induced Bifurcations in Systems with Impacts and Friction", International Journal of Non-Linear Mechanics, Vol. 44, 1011-1023.

[6] Genot, F. and Brogliato, B. (1999), "New Results on Painlevé Paradox", Eur. J.Mech. A/Solids Vol. 18, 653-677.
[7] Mason, M.T. and Wang, Y. (1988), "On the Inconsistency of Rigid-Body Frictional Planar Dynamics", Proceedings 1988 IEEE Int'l. Conf. Robotics and Automation, Philadelphia, 524-528.
[8] Pay, M. and Glocker C. (2005), "Oblique Frictional Impact of a Bar: Analysis and Comparison of Different Impact Law", Nonlinear Dyn. Vol 41, 361-383.
[9] Shen, Y. and Stronge, W., A. (2011), "Painleve Paradox during Oblique Impact with Friction", European Journal of Mechanics A/Solids, Vol. 30, 457-467.
[10] Leonesio, M. and Bianchi, G. (2009), "Self-Locking Analysis in Closed Kinematic Chains", Mechanism and Machine Theory, Vol. 44, 2038–2052
[11] Zhao, Z., Liu, C., Ma, W. and Chen, B. (2008), "Experimental Investigation of the Painlevé Paradox in a Robotic System", J. Appl. Mech., Vol. 75(4), 1-25.
[12] Elkaranshawy, H. and Ghazy, M. (2012), "Effect of the Link-Length Ratio on Painlevé Paradox for a Sliding Two-Link Robot", 15th International Conference on Applied Mechanics and Mechanical Engineering, Cairo, Egypt, RC 76-87.
[13] Ghazy, M. and Elkaranshawy, H. (2012), "A Method to Escape Painlevé Paradox in a Two-Link Robotic Manipulator." Proceedings of the International Conference on Engineering and Technology (ICET2012), New Cairo City, Egypt, 214-218.
[14] Elkaranshawy, H. (2011), "Using Self-Motion in Redundant Manipulators to Cope with Painleve Paradox," Proceedings of the IASTED International Conference on Robotics", Pittsburgh, USA, 361-367.